



**HAL**  
open science

## An urn model of the development of L/M cone ratios in human and macaque retinas.

Kenneth Knoblauch, Maureen Neitz, Jay Neitz

► **To cite this version:**

Kenneth Knoblauch, Maureen Neitz, Jay Neitz. An urn model of the development of L/M cone ratios in human and macaque retinas.. *Visual Neuroscience*, 2006, 23 (3-4), pp.387-94. 10.1017/S0952523806233157 . inserm-00131744

**HAL Id: inserm-00131744**

**<https://inserm.hal.science/inserm-00131744>**

Submitted on 19 Feb 2007

**HAL** is a multi-disciplinary open access archive for the deposit and dissemination of scientific research documents, whether they are published or not. The documents may come from teaching and research institutions in France or abroad, or from public or private research centers.

L'archive ouverte pluridisciplinaire **HAL**, est destinée au dépôt et à la diffusion de documents scientifiques de niveau recherche, publiés ou non, émanant des établissements d'enseignement et de recherche français ou étrangers, des laboratoires publics ou privés.

An urn model of the development of L/M cone ratios  
in human and macaque retinas

Kenneth Knoblauch<sup>1,2</sup>, Maureen Neitz<sup>3</sup>, Jay Neitz<sup>3</sup>

(January 19, 2006)

<sup>1</sup>Inserm, U371, Cerveau et Vision, Department of Cognitive Neuroscience, Bron F-69500, France;

<sup>2</sup>Université Claude Bernard Lyon 1, Institut Fédératif des Neurosciences (IFR 19), Bron cedex, F-69675, France

<sup>3</sup>Department of Cell Biology, Neurobiology, and Anatomy and Department of Ophthalmology, Medical College of Wisconsin, 8701 Watertown Plank Road, Milwaukee, WI 53226, USA

Corresponding author: Kenneth Knoblauch

Inserm U371, Cerveau et Vision  
Department of Cognitive Neuroscience  
18 avenue du Doyen Lépine  
69500 Bron  
France  
tel: +33 (0)4 72 91 34 77  
fax: +33 (0)4 72 91 34 61  
email: knoblauch@lyon.inserm.fr

Running Title: Human and macaque development of L/M cone ratios

Number of manuscript pages: 21

Number of tables: 0

Number of figures: 4

# An urn model of the development of L/M cone ratios in human and macaque retinas

## Abstract

A model is presented of the development of  $L/M$  cone ratios in the Old World primate retina. It is supposed that during gestation, the cone cycles randomly between states in which it transcribes either  $L$  or  $M$  opsin. The current state determines and increases the probability that it will transcribe the same opsin in future cycles. These assumptions are sufficient to formalize the process as a Markov chain that can be modeled as an urn containing two types of balls,  $L$  and  $M$ . Drawing one ball results in the increase of its species and the decrease of the other. Over the long run, the urn will become populated with a single type of ball. This state corresponds to the photoreceptor adopting a fixed identity for its lifetime. We investigate the effect of the number of states and the rule that regulates the advantage of transition toward one cone type or another on the relation between fetal and adult  $L/M$  cone ratios. In the range of 100 to 1000 states, small variations of the initial  $L/M$  ratio or the transition advantage can each generate large changes in the final  $L/M$  ratio, in qualitative accord with the variation seen in human adult retinas. The time course to attain stable  $L/M$  ratios also varies with these parameters. If it is supposed that the cycling follows a circadian rhythm, then final  $L/M$  cone ratios would be expected to stabilize shortly after birth in both human and macaque.

**Key Words:** L/M cone ratio, primate retinal development, color vision, Markov chain, urn model

## Introduction

In many species of New World primate, the presence of polymorphic variants of the single cone opsin gene on the X-chromosome allows heterozygous females to have trichromatic color vision (Jacobs et al., 1993). Different alleles of the gene encode photopigments with distinct spectral sensitivities, including variants that are nearly identical to the long- (*L*) and middle-wavelength (*M*) sensitive cone photopigments found in humans (Mollon et al., 1984). In each female cell, a stochastic dosage compensation mechanism, X-inactivation, maintains expression of the visual pigment from only one of the two X-chromosomes, thereby segregating expression of different alleles to separate populations of cones. Thus, in a New World primate trichromatic female the *L* or *M* fate of an incipient *LM* cone is determined by the allele on the X-chromosome that is chosen to remain active.

In contrast, in modern Old World (OW) primates both males and females enjoy trichromatic color vision. This is a consequence of a combination of gene divergence and duplication in an ancestor to OW primates that placed *L* and *M* genes in tandem on the same X-chromosome (Nathans et al., 1986). Since the *L* and *M* genes are on the same chromosome, OW primates must exploit some other mechanism besides X-inactivation to segregate expression of the *L* and *M* opsin genes to separate populations of cones. There is evidence that the mechanism involves a DNA element, positioned upstream of the X-chromosome, that is essential for expression of the *L* and *M* opsin genes (Nathans et al., 1989; Wang et al., 1992). DNA elements that facilitate transcription at a distance from the promoter are referred to as enhancers. The enhancer associated with the X-chromosome pigment gene in the OW primate ancestor was not duplicated in the evolutionary event that placed two pigment genes in tandem. Since, in OW primates

there is only one enhancer shared by both *L* and *M* genes at the locus it has been called the locus control region (LCR). The shared single enhancer can interact with only one opsin promoter at a time; thus, only one X-chromosome visual pigment gene will be transcribed at any one moment. However, enhancer/promoter interactions are dynamic, associating, dissociating and re-associating over time making it possible to express both *L* and *M* pigments in a single cone cell provided that the half-life of the pigment is long compared to the time required to disassociate and re-associate. In adult humans, *L* and *M* gene expression is mutually exclusive, presumably until death, implying that in the adult there is a mechanism that allows the LCR to associate with only one, *L* or *M*, opsin gene promoter in any one cone photoreceptor (Hagstrom et al., 2000).

Some of the details known about the *LM* cone mosaic in humans and nonhuman primates provide information to constrain the possible mechanisms that can be proposed to explain how the individual *L* and *M* cones differentiate to exclusively express a single opsin. The distribution of *L* and *M* cones is approximately random in the fovea, however a tendency toward clumping has been observed, and is more pronounced in the peripheral retina (Bowmaker et al., 2003; Carroll et al., 2002; Hofer et al., 2005; Packer et al., 1996; Roorda et al., 2001; Roorda & Williams, 1999). Strikingly, the *L/M* cone ratio varies widely between individuals (Carroll et al., 2002; Hofer et al., 2005; Roorda & Williams, 1999; Rushton & Baker, 1964). In humans the *L/M* ratio ranges from about 1/3 to 20/1 with an average of about 2/1 (Carroll et al., 2002). Although less information is available for macaques, the average ratio is nearer 1/1 and the range of variability may be smaller than in humans (Baylor et al., 1987; Bowmaker et al., 1983; Harosi, 1987; Marc & Sperling, 1977; Mollon & Bowmaker, 1992; Roorda et al., 2001).

A very important clue about the mechanism that dictates exclusive opsin expression in adult *L* and *M* cones comes from recent studies in the developing human

and macaque retina. Surprisingly, in fetal human retinas the  $L/M$  mRNA ratio is reversed compared to the ratio observed in adult retinas (McMahon et al., 2000; McMahon, Hendrickson, Neitz & Neitz, in preparation). The average percentage of  $L$  plus  $M$  messenger RNA (mRNA) that is  $L$  ( $\%L = 100 * L/[L + M]$ ) for the adult human retina was 66%  $L$  (or a 2/1 ratio of  $L/M$ ), whereas for the fetal retinas between 10.1 and 22 weeks of gestation, the average was 33%  $L$  (or a 1/2 ratio). A similar relationship between adult and fetal macaque mRNA ratios was also observed. At the fetal ages tested, all the nascent cones are present (LaVail et al., 1991) and few will be lost through cell death (Cornish et al., 2004). As assayed by immunohistochemistry there is roughly uniform expression of opsin in all the nascent  $LM$  cones (Cornish et al., 2004). The cones are redistributed as the adult retinal mosaic develops; however, in the absence of significant addition or loss of cones, cone migration cannot account for the difference in %L mRNA between fetal and adult retinas. Thus, the dramatic change in mRNA during development cannot be explained by gain or loss of one population of cones or a change in the amount of opsin transcribed in one class of cones. The only explanation that remains is that the relative amounts of  $L$  versus  $M$  mRNA must be changing within individual cones during development. Mechanistically, the simplest explanation is that during development, as the LCR associates, dissociates, and re-associates with the opsin gene promoters, it is free to choose either  $L$  or  $M$ , whereas in the adult its choice is restricted to the same opsin gene every time.

A key process of cellular differentiation is chromatin modification that silences gene transcription by incorporating DNA into heterochromatin, thereby restricting transcription to only those genes that give the cell its characteristic adult phenotype and function (Grewal & Moazed, 2003; Ringrose & Paro, 2004). Thus, it is reasonable to suppose that during photoreceptor development, all but one of the X-chromosome opsin

genes are silenced. The choice of which gene remains active versus which are silenced is hypothesized to involve a competition between the dynamic LCR/promoter interactions that facilitate transcription of the *L* and *M* genes and epigenetic transcriptional silencing modifications that are initially reversible but eventually become irreversible (McMahon et al., in preparation). For example, each time the LCR associates with one of the X-chromosome visual pigment gene promoters, the other genes in the array may be exposed to chromatin modifications that diminish their future ability to successfully compete for interaction with the LCR. The key feature of this hypothesis is that over the course of development, the probability that the LCR will associate with a given promoter constantly changes as a function of previous LCR/promoter associations, until finally all but one of the genes have accumulated so many chromatin modifications that their ability to attract the LCR is reduced to zero. At this point, the identity of the cone as *L* or *M* is determined and it will correspond to the opsin gene (*M* or *L*) that remains actively transcribed. It is predicted that genetically encoded differences in the initial ability of the *L* versus *M* promoters to recruit the LCR and in the susceptibility of the *L* versus *M* genes to silencing mechanisms would influence the final adult ratio of *L/M* cones and explain individual differences in the normal population. Such differences are likely to be genetically encoded in the form of DNA nucleotide polymorphisms at the X-chromosome opsin gene locus (McMahon et al., 2003; Smallwood et al., 2002).

This hypothesis can be modeled as a Markov Chain (Chung, 1974; Feller, 1968). A Markov Chain is constructed from a set of mutually exclusive states and a set of probabilities for changing between them. The fundamental property that defines a Markov Chain is that the probability of changing state depends only on the current state. At the simplest level, one can imagine the states as corresponding to the LCR associating with either the *L* or *M* gene promoter regions, but more elaborate schemes

can be considered in which the number of states refers to the probability of making the same coupling at subsequent times. In this article, we develop such a model and examine its properties with respect to explaining fetal and adult  $L/M$  cone ratios and adult variability in cone ratio.

## An urn model of the LCR-promoter interaction

We begin by constructing a physical model that incorporates the hypothesized characteristics of the competitive processes that activate versus silence transcription of the  $L$  and  $M$  opsin genes. Consider an urn filled with two types of balls labeled  $L$  and  $M$ , where an urn represents an individual developing  $LM$  photoreceptor, and the retina is a collection of urns. We will assume that the total number of balls in each urn is fixed,  $N$ . The number of  $L$  balls,  $n_L$ , determines the probability that an  $L$  or  $M$  ball will be drawn. Drawing a ball represents the photoreceptors choice to transcribe an  $L$  or  $M$  gene. By analogy, the proportion  $n_L/N$  can be taken as the initial probability that the  $L$  gene will be chosen for transcription by associating with the LCR ( $1 - n_L/N$ , the probability of associating with the  $M$  promoter). If this initial choice is made independently within each photoreceptor, then these probabilities can also be taken to represent the initial proportions of photoreceptors transcribing an  $L$  versus an  $M$  opsin gene as reflected in the % $L$  mRNA in fetal retina. Note that, in adult photoreceptors, cone opsin gene transcription oscillates on a diurnal rhythm, with negligible amounts of mRNA from one round still remaining when the next round of transcription begins (von Schantz et al., 1999). If this holds true in development, as seems likely, then cones can be labeled as  $L$  or  $M$  according to the opsin gene being transcribed.

Suppose now that we adopt a rule that each time an  $L$  ball is drawn from an urn,  $r$

additional  $L$  balls will be added and  $r$   $M$  balls removed. Similarly, each time an  $M$  ball is drawn,  $s$  additional  $M$  balls are added and  $s$   $L$  balls removed. We will refer to the ratio  $r : s$  as the  $L:M$  advantage (which we distinguish from the ratio of  $L$  to  $M$  cones, indicated throughout this article by the fraction  $L/M$ ). Over time the contents of each urn will change, influencing the future probability of choosing an  $L$  versus an  $M$  ball. Because  $r$  and  $s$  are positive integers, each time a particular type of ball is chosen, the probability increases for subsequent draws to be balls of the same type. In the long run, each urn will become entirely populated with one type of ball at the exclusion of the other, and no further changes in its composition can occur. The replacement rule is taken to reflect the process by which association of the LCR with a particular opsin gene promoter increases the probability of subsequent associations with that same promoter because the associated gene is protected and the other genes are exposed to silencing mechanisms. When an urn becomes filled with balls of only one type, this is akin to the silencing of all but one of the opsin genes so that one remains viable for transcription.

The urn model described above can be represented by a Markov chain with  $N + 1$  mutually exclusive states, corresponding to the urn containing from 0 to  $N$   $L$  balls. If after a certain draw, the urn contains  $n_L$   $L$  balls and  $N - n_L$   $M$ , then the probability that it will contain  $n_L + r$   $L$  balls on the next draw is  $n_L/N$  and the probability that it will contain  $n_L - s$   $L$  balls is  $1 - n_L/N$ . Since all other states are unreachable in one draw from this state, their probabilities are 0. This description provides the rule for filling a transition matrix that indicates the probabilities of changing between any two states.

To give a simple example, consider a 10 ball urn that initially contains 6  $L$  and 4  $M$  balls. Take the rule as that an  $L$  draw adds 3  $L$  and removes 3  $M$  balls, and an  $M$  draw results in adding 1  $M$ , eliminating the same number of  $L$ . The transition matrix is

	[10]	[9]	[8]	[7]	[6]	[5]	[4]	[3]	[2]	[1]	[0]
[10]	1.0	0.0	0.0	0.0	0.0	0.0	0.0	0.0	0.0	0.0	0.0
[9]	0.9	0.0	0.1	0.0	0.0	0.0	0.0	0.0	0.0	0.0	0.0
[8]	0.8	0.0	0.0	0.2	0.0	0.0	0.0	0.0	0.0	0.0	0.0
[7]	0.7	0.0	0.0	0.0	0.3	0.0	0.0	0.0	0.0	0.0	0.0
[6]	0.0	0.6	0.0	0.0	0.0	0.4	0.0	0.0	0.0	0.0	0.0
[5]	0.0	0.0	0.5	0.0	0.0	0.0	0.5	0.0	0.0	0.0	0.0
[4]	0.0	0.0	0.0	0.4	0.0	0.0	0.0	0.6	0.0	0.0	0.0
[3]	0.0	0.0	0.0	0.0	0.3	0.0	0.0	0.0	0.7	0.0	0.0
[2]	0.0	0.0	0.0	0.0	0.0	0.2	0.0	0.0	0.0	0.8	0.0
[1]	0.0	0.0	0.0	0.0	0.0	0.0	0.1	0.0	0.0	0.0	0.9
[0]	0.0	0.0	0.0	0.0	0.0	0.0	0.0	0.0	0.0	0.0	1.0

The row labels in brackets indicate current possible states (number of  $L$  balls), the column labels indicate future possible states. The transition probabilities fill the matrix. When the urn has 6  $L$  balls, the row labeled [6] indicates that there is a 0.6 probability that the subsequent state will contain 9  $L$  balls and a 0.4 probability that it will contain 5. The unit values in the upper left and lower right diagonal slots indicate urns with only one type of ball. These are called absorption states since once an urn reaches one of these states, it stays there forever. Recalling that the urn model represents the competitive processes within an individual developing photoreceptor between activation and silencing of the X-chromosome opsin gene transcription, and the absorption states indicate conditions when the photoreceptor becomes committed to transcribing a specific opsin gene.

To follow the evolution of the system, consider as input a row vector with all 0's

and a 1 in one place, for example,

$$v_0 = (0, 0, 0, 0, 1, 0, 0, 0, 0, 0).$$

The 1 in the fifth place indicates that there are 6  $L$  balls in the urn (fifth row from top of matrix). Let the transition matrix above be denoted by  $M$ . Then, the probability distribution of balls after the next draw is

$$v_0 \cdot M = v_1 = (0, 0.6, 0, 0, 0, 0.4, 0, 0, 0, 0).$$

The distribution for the second draw is

$$v_2 = v_1 \cdot M = v_0 \cdot M^2 = (0.54, 0, 0.26, 0, 0, 0.2, 0, 0, 0, 0).$$

In general, the distribution on the  $n^{\text{th}}$  draw will be  $v_n = v_0 \cdot M^n$ . The limiting equilibrium distribution will be attained as  $n$  approaches  $\infty$ . The matrix  $M^n$  approaches a limiting form, given in this case by

	[10]	[9]	[8]	[7]	[6]	[5]	[4]	[3]	[2]	[1]	[0]
[10]	1.000	0	0	0	0	0	0	0	0	0	0.000
[9]	1.000	0	0	0	0	0	0	0	0	0	0.000
[8]	0.996	0	0	0	0	0	0	0	0	0	0.004
[7]	0.979	0	0	0	0	0	0	0	0	0	0.021
[6]	0.929	0	0	0	0	0	0	0	0	0	0.071
[5]	0.823	0	0	0	0	0	0	0	0	0	0.177
[4]	0.650	0	0	0	0	0	0	0	0	0	0.350
[3]	0.430	0	0	0	0	0	0	0	0	0	0.570
[2]	0.216	0	0	0	0	0	0	0	0	0	0.784
[1]	0.065	0	0	0	0	0	0	0	0	0	0.935
[0]	0.000	0	0	0	0	0	0	0	0	0	1.000

Note that in the limiting case only the first and last columns contain non-zero values. The first (last) column indicates the probability of an all  $L$  ( $M$ ) urn given the initial number of  $L$  balls indicated in brackets for each row. The solid black curve in Figure 1 shows that this relation is sigmoidal. As expected intuitively, the greater the initial number of  $L$  balls in the urn, the more likely the urn will finish filled with  $L$  balls or, by analogy, that the cone will henceforth only transcribe an  $L$  opsin gene. If an equivalent competitive process occurs independently in each cone, then the curves indicate the final proportion of cones transcribing an  $L$  gene as a function of the initial % $L$  mRNA. Thus, in this system, with an initial % $L$  mRNA of 0.4, the expected final proportion of  $L$  cones is 0.65. Changing the rule to one in which drawing an  $L$  ball results in the addition of only 1 or 2  $L$  balls generates the dashed and dotted curves in Figure 1, respectively, that are simply translated to the right along the abscissa. The above small

example illustrates the basic mechanism of this model. In the rest of this article, we explore its characteristics for a larger number of states, the effect of different ball-replacement rules on the variability of the final state and the time requirements for the system to reach equilibrium. All calculations were performed using the R statistical computing language and environment (R Development Core Team, 2005). The code is available on request from the first author.

Figure 1 about here

## Results

Figures 2a and b illustrate how the final proportion of  $L$  cones in the retina is related to the initial proportion for different  $L:M$  advantages for (a) 101 state (100 ball) and (b) 1001 state (1000 ball) systems. As with the 11 state system, changing the  $L:M$  advantage only causes lateral shifts of the curves. Changing the number of states, however, generates steeper curves. Intuitively, the number of balls in the urn determines how big an effect on the composition of the urn the replacement rule will have after each draw, and therefore how much the probability of drawing an  $L$  ball will change after each draw. In this model, the number of states has an inverse influence on the size of the increment step in probability of re-associating with the same promoter each time the enhancer disassociates. The gray solid and dotted lines in Fig. 2 connect initial and final % $L$  opsin mRNA estimates from human and macaque data, respectively, to indicate which curve best predicts the data for each species. The initial % $L$  was taken as the average % $L$  opsin mRNA observed for fetal retinas, 0.18 for macaques and 0.33 for humans (McMahon et al., 2000; McMahon et al., in preparation), and this reflects the greater ability of the  $M$  gene promoter to attract the LCR compared to the  $L$

promoter (Smallwood et al., 2002). The final % $L$  was taken as 0.55 for macaques, reflecting the average of the estimates in the literature for this species (Baylor et al., 1987; Bowmaker et al., 1983; Harosi, 1987; Roorda et al., 2001), and 0.67 for humans (Carroll et al., 2002; Hagstrom et al., 1998; McMahon et al., in preparation). For 101 states, macaques require an 8:1  $L:M$  advantage whereas a value closer to 2.5:1 works better for human. For 1001 states, the macaque would require a 6:1 advantage and humans would require close to 2.25:1. It is not unexpected that macaques and humans would differ in the  $L:M$  advantage considering that they differ in the number and locations of nucleotide polymorphisms at the opsin gene locus, including in the  $L$  and  $M$  gene promoters (McMahon et al., 2003). In addition, the  $L$  and  $M$  genes are each flanked by unique DNA sequences so that each opsin gene occupies a unique chromatin environment, hence the  $L$  and  $M$  genes may not be equally susceptible to silencing even across individuals within a species. In general, the lower initial  $L$  opsin expression in fetal macaque retinas requires a greater  $L:M$  advantage to attain the adult values. The steepness of all curves indicates that relatively small changes in the initial % $L$  cones could generate large changes in the final values.

Figure 2 about here

It should be noted that an  $L:M$  advantage of 2:1 does not produce the same results as one with 4:2. The latter gives a shallower curve with the same slope as the curves from a system with half of the number of states but using a 2:1 advantage. Intuitively, the 4:2 advantage only uses half of the states of the system, for example, systematically skipping odd-labeled states if starting from an even-labeled state. This observation is what permitted the calculation of curves for non-integer  $L:M$  advantages. Thus, the curve for the 2.5:1  $L:M$  advantage in Figure 2a is obtained by evaluating a 201 state

system with a 5:2  $L:M$  advantage. Note that this curve has the same slope as the others in the figure and falls intermediate between the 2:1 and 3:1 curves.

Figures 3a–d illustrate how the final % $L$  cones varies as a function of the  $L:M$  advantage. Only the numerator of the  $L:M$  advantage is indicated on the abscissas. These curves were obtained by taking vertical slices through those in Figure 2 at the human and macaque initial % $L$  cone values. Note the differences in the axes scalings. Figures 3a and b indicate human and macaque values, respectively, for the 101 state system. Figures 3c and d display the same for the 1001 state system. The dashed lines in Figure 3a show that in humans a change in the advantage from 2:1 to 4:1 can push the system from a final  $L/M$  ratio of 1/3 to nearly 20/1. Thus, small changes in the propensity of the LCR to associate with the individual promoters could generate very large changes in the  $L/M$  ratio in the retina. In the 1001 state system, even smaller changes can result in the same final variation. Interestingly, the 101 state system for the macaque initial conditions seems to asymptote near 70%  $L$  (Figure 3b). The origins of this phenomenon can be seen in Figure 2a, in which the leftward displacements of the curves diminish as the  $L:M$  advantage increases. It seems to result from the extreme initial % $L$  values in fetal macaques and when the step-size implied by the large  $L:M$  advantage approaches the number of states in the system. Speculatively, if this number of states were to characterize the macaque  $L$  and  $M$  cones, then it would predict that the range of variation in the  $L/M$  ratios across animals would be narrower than in human. For example, a two-fold variation in the  $L:M$  advantage, indicated by the dashed lines in Figure 3b, results in only a two-fold change in the  $L/M$  ratio, compared to the 60-fold change in the human. This finding is consistent with reports in the literature (Baylor et al., 1987; Bowmaker et al., 1983; Harosi, 1987; Marc & Sperling, 1977; Mollon & Bowmaker, 1992; Roorda et al., 2001); however, we must await more

experimental data to evaluate whether the true range of variation in  $L/M$  ratio in macaques is actually reduced compared to humans. In any case, increasing the number of states would eliminate this phenomenon as shown in Figure 3d.

Figure 3 about here

Finally, it is possible to follow the evolution of the probabilities of the system and the time frame over which cones become committed to the two absorption states, transcribing solely an  $L$  or an  $M$  gene, by repeated multiplication of the input vector by the transition matrix. Interpretation of the time scale requires knowledge of the periodicity of associations between the LCR and an opsin gene promoter. There is evidence that rod and cone opsin gene transcription is under circadian control (Rajendran et al., 1996; von Schantz et al., 1999) For example, in the adult mouse, UV cone opsin mRNA oscillates on a diurnal rhythm that is maintained even under constant darkness, as characteristic of genes under circadian control (von Schantz et al., 1999). If fetal primate cone opsin is also under circadian control during development, then the time step would correspond to one day. Figures 4a–d show the number of time steps (matrix multiplications) required for 99% of the cones to be committed to transcribing either an  $L$  or an  $M$  opsin gene for human and macaque initial %L cone values for 101 and 1001 states systems. Note the differences in scale of the abscissa on each figure. Each curve begins with a flat portion during which the cones are cycling with the LCR associating, dissociating and re-associating with the  $L$  or  $M$  opsin gene promoters. After this period, the number of cones transcribing only one opsin gene rises rapidly and begins to level off after about 80% of the cones have committed to transcribing either one or the other opsin. In general, the 101 state system (a and b) requires fewer steps to achieve 99% commitment than the 1001 state system (c and d),

and the human initial conditions (a and c) result in a greater number of steps than those of the macaque (b and d). For the human initial conditions, the 101 state system requires 181 days for 99% commitment, while the macaque requires only 68 days. The 1001 state systems predict much longer periods, with 1073 and 2301 days for the macaque and humans, respectively to achieve the criterion level.

Figure 4 about here

## Discussion

The urn model that we exploit resembles the Ehrenfest model (Chung, 1974) used in modeling equilibria of gas mixtures. The principal difference is that here the quantities  $r$  and  $s$ , the number of balls replaced at each draw, are non-negative integers, whereas in the Ehrenfest model, they are non-positive. Over time, an Ehrenfest urn approaches an equilibrium ratio of ball types, rather than performing as a winner-take-all mechanism, as here. Another feature of the model is that the number of balls is fixed. One reason for this is that if we let  $N$  vary as in, for example, a Polya urn model, the probabilities would depend on  $N$  and would no longer be described simply by a Markov chain in which the probabilities only depend on the current state (Chung, 1974). A fixed number of balls could represent a fixed area of DNA on which the LCR and gene silencing mechanisms act to facilitate or silence opsin gene transcription.

We have illustrated how a Markov chain based on an urn model could characterize a competition during development between activation and silencing of opsin gene transcription to arrive at stable transcription of an  $L$  or  $M$  gene in macaque and human cones. Our present knowledge of the developmental expression pattern of the opsin genes and the LCR's role in mediating transcription of these genes is consistent with the

characteristics of the Markov Chain Urn paradigm. Interestingly, for the 101 state systems for man and monkey, the paradigm predicts that all photoreceptors will have achieved an absorption state very near the time of birth assuming that the LCR disassociates once per day. Humans have a gestational period of about 270 days, and the 101 states system required 181 days to achieve an absorption state when starting with a %*L* mRNA value of 0.33. The process would be complete by about 335 days, or about 2 months after birth. Similarly, for macaques, a previous study showed that average %*L* mRNA was 0.18 for three fetal time points, fetal days 122, 123, and 144. Macaques have a 165 day gestation period, and the 100 states system required 68 days to achieve an absorption state from an initial state of 0.18. Thus, for the macaque the process would be complete by approximately a month after birth.

Smallwood and colleagues (2002) proposed that variation in the DNA sequences of the *L* and *M* gene promoters may contribute to variation in the *L/M* cone ratio by altering the relative abilities of the two promoters to bind to the LCR. The Markov Chain Urn paradigm provides support for this concept. This is of particular interest because, in a previous study to test the hypothesis that *L/M* cone ratio variation in humans is correlated to variation in the DNA sequence of the *L* and *M* gene promoters, it was discovered that, although there is very little sequence variation in the promoters among humans with normal color vision, the two variants identified were both associated with extreme *L/M* cone ratios (McMahon et al., 2004).

Previous studies have shown there to be variation in the topographical distribution of *L/M* cone ratios, with the peripheral human retina having a significantly higher ratio compared to the fovea (Hagstrom et al., 1998; M. Neitz et al., submitted to this issue). Thus, the fovea and peripheral retina cannot be modeled with the same urn. Different urn parameters would be required to model the development of the adult peripheral

retina, most significantly, the starting value for the ratio of L to M balls in the urn, and the number of states required to reach the adult ratio of L/M cones in the adult peripheral retina. One intriguing observation made using the urn model is that very small changes in urn parameters produce relatively large differences in the final L/M ratios achieved. This is exactly what would be needed to produce the variability in the L/M ratio across individuals, and as a function of retinal eccentricity.

## Acknowledgment

This work was supported by NIH grants EY09620, EY01931 and by Research to Prevent Blindness.

## References

- Baylor D.A., Nunn B.J. & Schnapf J.L. (1987), Spectral sensitivity of cones of the monkey *Macaca fascicularis*, J Physiol, 390, 145–160.
- Bowmaker J.K., Mollon J.D. & Jacobs G.H. (1983), Microspectrophotometric results for old and new world primates, in Colour Vision, eds. J.D. Mollon & L.T. Sharpe, London: Academic Press, pp. 57–68.
- Bowmaker J.K., Parry J.W.L. & Mollon J.D. (2003), The arrangement of L and M cones in human and a primate retina, in Normal and Defective Colour Vision., eds. J.D. Mollon, J. Pokorny & K. Knoblauch, New York: Oxford University Press, pp. 39–50.
- Carroll J., Neitz J. & Neitz M. (2002), Estimates of L:M cone ratio from ERG flicker photometry and genetics, J Vis, 2, 531–542.
- Chung K.L. (1974), Elementary Probability Theory with Stochastic Processes, New York: Springer-Verlag.
- Cornish E.E., Xiao M., Yang Z., Provis J.M. & Hendrickson A.E. (2004), The role of opsin expression and apoptosis in determination of cone types in human retina, Exp Eye Res, 78, 1143–1154.
- Feller W. (1968), An Introduction to Probability Theory and Its Applications, Volume 1, New York: John Wiley & Sons, Inc., third edition.
- Grewal S.I.S. & Moazed D. (2003), Heterochromatin and epigenetic control of gene expression, Science, 301, 798–802.

- Hagstrom S.A., Neitz J. & Neitz M. (1998), Variations in cone populations for red-green color vision examined by analysis of mRNA, Neuroreport, 9, 1963–1967.
- Hagstrom S.A., Neitz M. & Neitz J. (2000), Cone pigment gene expression in individual photoreceptors and the chromatic topography of the retina, J Opt Soc Am A Opt Image Sci Vis, 17, 527–537.
- Harosi F.I. (1987), Cynomolgus and rhesus monkey visual pigments. Application of Fourier transform smoothing and statistical techniques to the determination of spectral parameters, J Gen Physiol, 89, 717–743.
- Hofer H., Carroll J., Neitz J., Neitz M. & Williams D.R. (2005), Organization of the human trichromatic cone mosaic, J Neurosci, 25, 9669–9679.
- Jacobs G.H., Neitz J. & Neitz M. (1993), Genetic basis of polymorphism in the color vision of platyrrhine monkeys, Vision Res, 33, 269–274.
- LaVail M.M., Rapaport D.H. & Rakic P. (1991), Cytogenesis in the monkey retina, J Comp Neur, 309, 86–114.
- Marc R.E. & Sperling H.G. (1977), Chromatic organization of primate cones, Science, 196, 454–456.
- McMahon C., Hendrickson A.E., Dacey D.M., Neitz J. & Neitz M. (2000), L:M cone ratio as a function of eccentricity in primate retina estimated from analysis of messenger RNA [ARVO abstract], Invest Ophthalmol Vis Sci, 41, S494.
- McMahon C., Neitz J. & Neitz M. (2003), Comparison of human and monkey pigment gene promoters to evaluate DNA sequences proposed to govern L:M cone ratio, in

Normal & Defective Colour Vision, eds. J.D. Mollon, J. Pokorny & K. Knoblauch, Oxford: Oxford University Press, pp. 51–59.

McMahon C., Neitz J. & Neitz M. (2004), Evaluating the human X-chromosome pigment gene promoter sequences as predictors of L:M cone ratio variation, J Vis, 4, 203–208.

Mollon J.D. & Bowmaker J.K. (1992), The spatial arrangement of cones in the primate fovea, Nature, 360, 677–679.

Mollon J.D., Bowmaker J.K. & Jacobs G.H. (1984), Variations of colour vision in a New World primate can be explained by polymorphism of retinal photopigments, Proc R Soc Lond B Biol Sci, 222, 373–399.

Nathans J., Davenport C.M., Maumenee I.H., Lewis R.A., Hejtmancik J.F., Litt M., Lovrien E., Weleber R., Bachynski B. & Zwas F. (1989), Molecular genetics of human blue cone monochromacy, Science, 245, 831–838.

Nathans J., Piantanida T.P., Eddy R.L., Shows T.B. & Hogness D.S. (1986), Molecular genetics of inherited variation in human color vision, Science, 232, 203–210.

Packer O.S., Williams D.R. & Bensinger D.G. (1996), Photopigment transmittance imaging of the primate photoreceptor mosaic, J Neurosci, 16, 2251–2260.

R Development Core Team (2005), R: A language and environment for statistical computing, R Foundation for Statistical Computing, Vienna, Austria, URL <http://www.R-project.org>, ISBN 3-900051-07-0.

Rajendran R.R., Van Niel E.E., Stenkamp D.L., Cunningham L.L., Raymond P.A. &

Gonzalez-Fernandez F. (1996), Zebrafish interphotoreceptor retinoid-binding protein: differential circadian expression among cone subtypes, J Exp Biol, 199, 2775–2787.

Ringrose L. & Paro R. (2004), Epigenetic regulation of cellular memory by the Polycomb and Trithorax group proteins, Annu Rev Genet, 38, 413–443.

Roorda A., Metha A.B., Lennie P. & Williams D.R. (2001), Packing arrangement of the three cone classes in primate retina, Vision Res, 41, 1291–1306.

Roorda A. & Williams D.R. (1999), The arrangement of the three cone classes in the living human eye, Nature, 397, 520–522.

Rushton W.A. & Baker H.D. (1964), Red–green sensitivity in normal vision, Vision Res, 4, 75–85.

Smallwood P.M., Wang Y. & Nathans J. (2002), Role of a locus control region in the mutually exclusive expression of human red and green cone pigment genes, Proc Natl Acad Sci U S A, 99, 1008–1011.

von Schantz M., Lucas R.J. & Foster R.G. (1999), Circadian oscillation of photopigment transcript levels in the mouse retina, Brain Res Mol Brain Res, 72, 108–114.

Wang Y., Macke J.P., Merbs S.L., Zack D.J., Klaunberg B., Bennett J., Gearhart J. & Nathans J. (1992), A locus control region adjacent to the human red and green visual pigment genes, Neuron, 9, 429–440.

## Figure Legends

**Figure 1.** The probability that an urn of 10 balls of type  $L$  and  $M$  will reach an all  $L$  equilibrium as a function of the initial number of  $L$  balls in the urn, for three different replacement rules. The solid curve indicates a 3:1 advantage for each  $L$  draw. The dotted and dashed curves indicate advantages of 2:1 and 1:1, respectively.

**Figure 2.** The curves indicate the expected proportion of cones transcribing  $L$  opsin mRNA in the adult retina as a function of the initial fetal  $L$  transcription rate for a series of different  $L:M$  advantages (only the numerator of the advantage is displayed in the legends), given a competition between the LCR and promoter regions as described in the text. Part a indicates a model with 101 states and part b with 1001 states. The gray solid and dotted lines indicate for human and macaque, respectively, the initial and final average estimates of the percentage of cones transcribing the  $L$  opsin gene.

**Figure 3.** The curves show the expected proportion of cones transcribing  $L$  opsin mRNA in the adult retina as a function of  $L:M$  advantage. Only the numerator of the advantage is indicated on the abscissa. a. Human initial conditions for 101 states. b. Macaque initial conditions for 101 states. c. Human initial conditions for 1001 states. d. Macaque initial conditions for 1001 states. The dashed lines in a and b indicate the change in adult % $L$  mRNA for a factor of two change in the advantage around the value that most closely predicts the observed average fetal and adult values.

**Figure 4.** The curves show the expected proportion of cones that have committed to transcribing either an  $L$  or an  $M$  opsin gene as a function of the time step. The curves stop at the point that 99% of the cones have committed. a. Human initial conditions for 101 states. b. Macaque initial conditions for 101 states. c. Human initial conditions for 1001 states. d. Macaque initial conditions for 1001 states.

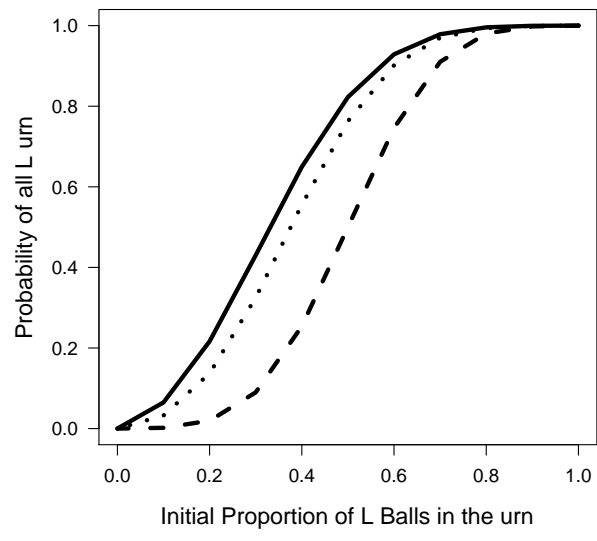
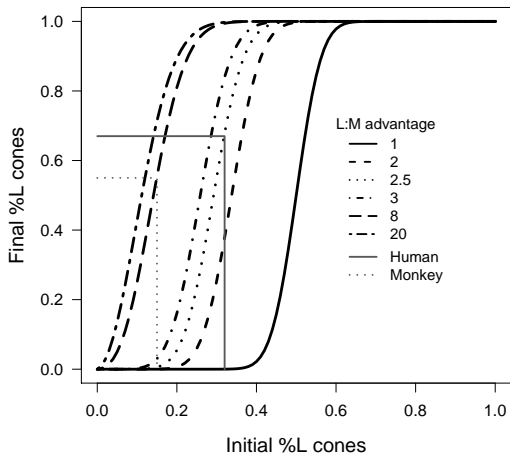


Figure 1

a



b

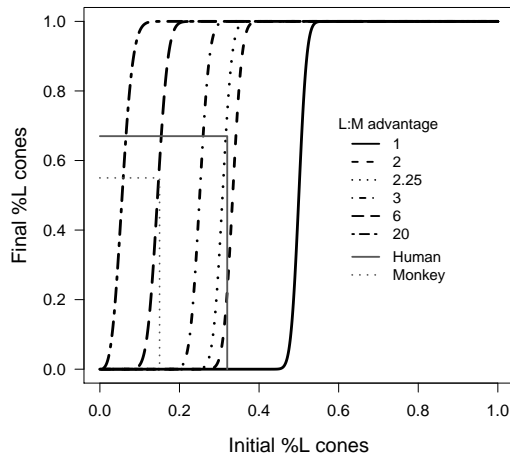
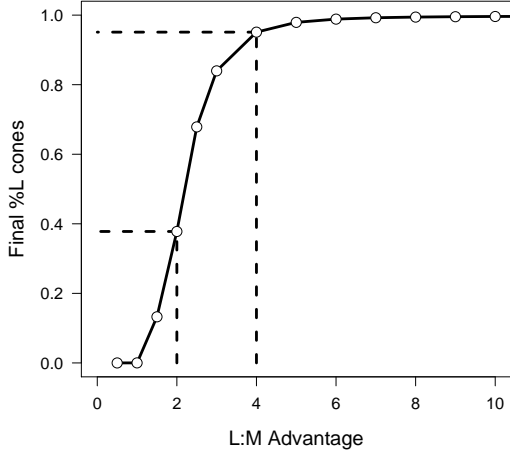
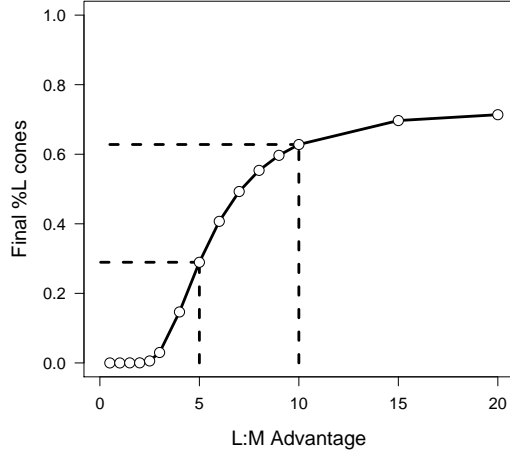


Figure 2

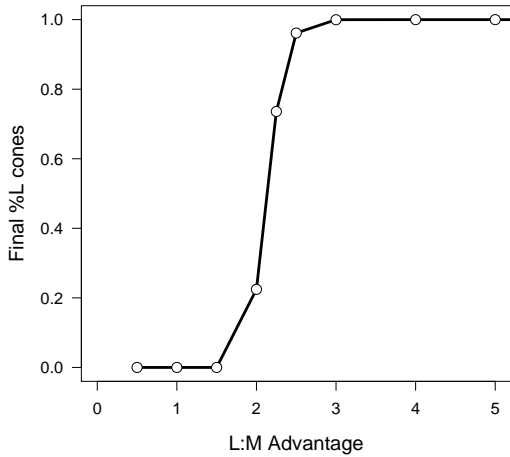
a



b



c



d

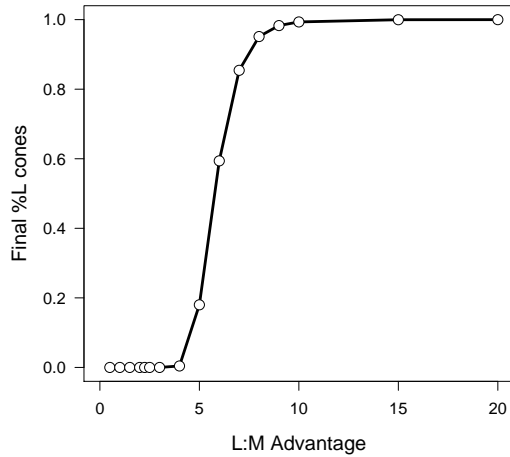
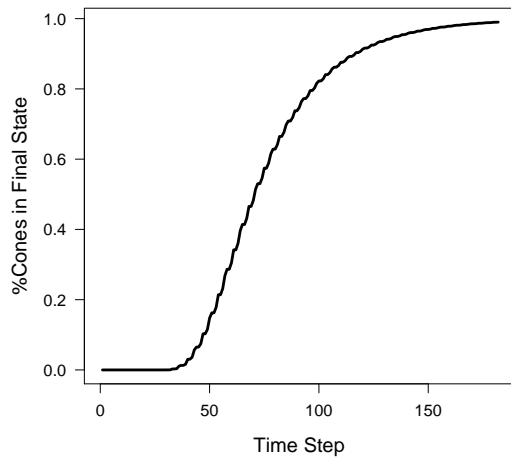
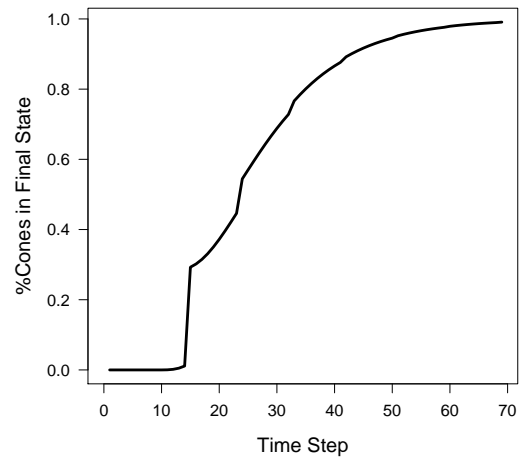


Figure 3

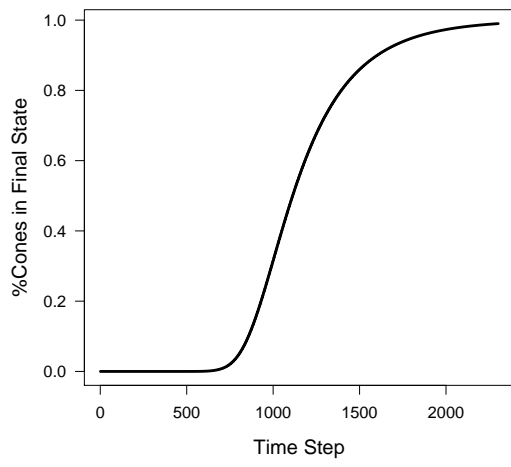
a



b



c



d

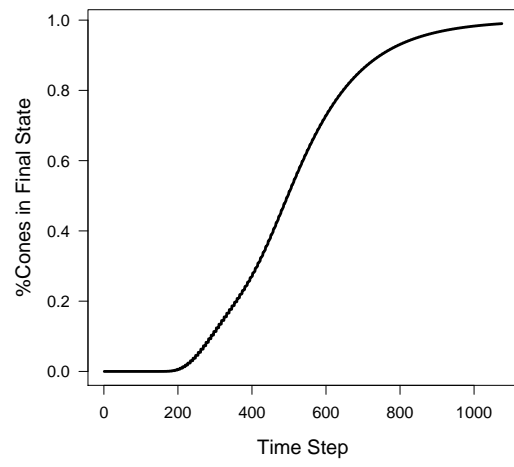


Figure 4